

is doubtful that the results could be explained by the larger volume load because the fish used in this study were proportionately larger than those used in previous studies. In the one small fish used in this study, a 100 ml volume load resulted in a sustained increase in dorsal aortic pressure. The magnitude of the dorsal aortic response appears to be more related to pre volume loading pressures than to the % of fish weight represented by the 250 ml of ringers. It is likely that the slight but significant increase in dorsal aortic pressure reported after volume loading (Kent, et al, MDIBL, 14:55, 1974) would have continued to increase if hemorrhage had not been superimposed. More difficult to explain is the lack of dorsal aortic pressure increase after volume loading by Solomon, et al., 1982. Perhaps pithing abolishes a neurogenic vascular tone.

In the present study changes in dorsal aortic pressure were mimicked in direction and time course by changes in rectal gland secretion rate. The increase in rectal gland secretion rate is a well documented phenomenon. The increase in rectal gland secretion rate after epinephrine is not expected from work on isolated perfused rectal glands where catecholamines were found to inhibit secretion (Shuttleworth and Thompson, Bull. MDIBL, 21:59, 1981). This result may indicate that in the intact fish epinephrine mediates the release of the purported hormone responsible for increased rectal gland secretion. It is also interesting that when volume load is followed by hemorrhage the rectal gland secretion rate response is reversed. The volume depletion may inhibit the release of the circulating factor causing increases in rectal gland secretion rate or perhaps a factor which turns off the secretory process is elaborated when circulating blood volume is lowered. After hemorrhage dorsal aortic pressure fell to a control value of 23 mmHg. This pressure should be adequate to perfuse the gland, but hemodynamic changes limiting rectal gland perfusion after hemorrhage cannot be ruled out as an explanation for the decrease in rectal gland secretion rate after blood loss. This work was supported by research funds from the Department of Surgery, Mt. Sinai School of Medicine, N.Y., N.Y., and by funds from NICHD project #AD16899. Mr. Bonilla was supported by a fellowship from the American Heart Association, Maine Affiliate and by the Medical Scientist Training Grant GMO7280, National Institute of General Medical Sciences through Mt. Sinai.

MECHANICS AND BIOCHEMISTRY OF ARTERIAL SEGMENTS FROM THE PREGNANT DOG FISH

E.O. Fuller, K.K. Griendling and B. Kent, Department of Physiology, University of Pennsylvania School of Medicine, Philadelphia, Pa., and Departments of Surgery and Physiology, Mt. Sinai School of Medicine, New York, N.Y.

The uterine artery enlarges markedly to accommodate the increase in blood flow that accompanies gestation. The effect of these changes on either the mechanical or biochemical characteristics of this artery has not been studied in the dogfish (*Squalus acanthus*). We therefore undertook a small number of experiments to characterize the in vitro responses of segments of the uterine artery to changes in pressure and to determine whether these changes differ from those of another systemic artery, the mesenteric. We also measured DNA and RNA content of the arteries as an indicator of growth.

Methods

Six pregnant female dogfish were anesthetized with Na pentobarbital (20 mg/kg body wt) and pithed between C₂ and C₅. Following a ventral mid-line incision, 2-4 cm segments of the uterine, mesenteric and rectal gland arteries were dissected free of connective tissue and placed in cold (6°C) Ringers solution (Kent, 1982) containing 11 mM glucose and gassed with 5% CO₂, 95% O₂. Segments were mounted horizontally on two needles in a muscle chamber. The artery was inflated with air introduced through one needle, while the other needle was coupled to a force transducer which monitored axial force (Cox, 1974). A cantilevered diameter transducer spanned the mid-section of the vessel to monitor diameter changes. Pressure-diameter curves were obtained by slowly varying pressure between 0-100 mm Hg, and recording diameter. This procedure was carried out under activated (in the

presence of phenylephrine 10^{-4} M and 122 mM K^{+}) and passive (in the presence of iodoacetate 10^{-5} M in low Ca^{++} (.1 mM), glucose-free buffer) conditions. Measurements of pressure, axial force, diameter and segment length, were used to calculate radial and tangential stress and the elastic modulus (Cox, RH, J. Appl. Physiol. 36:381-384, 1974) which characterize mechanical behavior of an artery. The remaining tissue was used to measure DNA (indole method, Ceriotti, G., J. Biol. Chem. 198: 297-303, 1952) and RNA (orcinol method, Dische, Z. and Schwarz, K., Mikrochim. Acta 2:13, 1937), and the dry/wet weight ratio.

Results

Because blood pressure in the ventral aorta of the dogfish is in the order of 20 mmHg (17, 25) these arteries were studied at pressures that ranged from 0 to 100 mmHg instead of the 0-300 mm Hg range used for most terrestrial mammals, and at a temperature of 16°C instead of the 37°C used for homeotherms. Activated and passive tension curves from the three uterine and two mesenteric arteries of dogfish in late pregnancy were generated. The shapes of the pressure-diameter curves from both the uterine and mesenteric arteries were similar to those recorded from rat carotid arteries (Cox, RH, Am. J. Physiol. 233:H256-H263, 1977) except that the entire curve was completed at pressures below 100 mm Hg. Figure 1 describes the relationship between active tangential stress (force/unit area applied in a circumferential direction) and normalized radius (the external radius normalized to the radius of the uninflated vessel) found in a typical uterine artery. Peak stress occurs when the radius is between 70 and 80% greater than its uninflated value. Figure 2 describes the relationship between active radial stress and strain in the

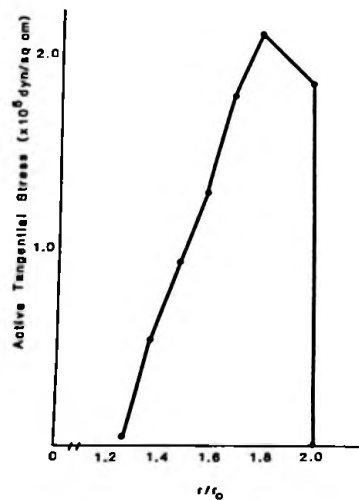


Figure 1.--Example of active circumferential stress-normalized radius curves for a pregnant uterine artery. Radius is normalized to the passive external radius at zero mm Hg (r/r_0)

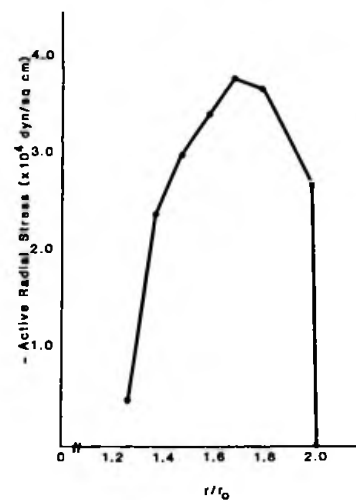


Figure 2.--Example of active radial stress-normalized radius for a pregnant uterine artery. Radius normalized as in Figure 1.

same artery. Radial stress is actually negative as it is a compressive rather than a tensile force. The shapes of the curves calculated for both the uterine and mesenteric arteries of the remaining fish were similar.

Selected mechanical data for the pregnant uterine and mesenteric arteries are presented in Table 1. The vessels were of similar size (r_0), but had very different radius to wall thickness ratios (r/h). The higher r/h of the mesenteric artery probably reflects both a larger external radius (r) and a thinner wall. Maximum circumferential stress ($\text{Max } \sigma_c$) was higher in the mesenteric than in the uterine artery, while maximum radial stress ($\text{Max } \sigma_r$) was similar in both arteries. The strains at which the maximums occurred were also similar. However,

Table 1.--Mechanical Data

	Uterine	Mesenteric
r_o (cm)	$0.44 \pm .002$ (3)	0.50 ± 0 (2)
r_{max}/r_o	$1.79 \pm .12$ (3)	2.00 ± 0 (2)
Max σ_c ($\times 10^5$ dyn/cm ²)	2.06 ± 1.512 (3)	$3.86 \pm .38$ (2)
Max σ_f ($\times 10^4$ dyn/cm ²)	$-3.16 \pm .33$ (3)	$-3.06 \pm .69$ (2)
Passive P=20 mmHg		
r (cm)	$.077 \pm .004$ (3)	$.099 \pm .003$ (2)
r/r_o	$1.76 \pm .09$ (3)	$1.98 \pm .06$ (2)
r/h	$3.53 \pm .93$ (3)	7.46 ± 1.4 (2)
E_{inc} ($\times 10^5$ dyn/cm ²)	9.27 ± 1.3 (3)	18.0 ± 3.5 (2)

Mean \pm SEM (n). r_o = radius at zero pressure in passive state. r_{max}/r_o = radius at which maximum active stress occurs normalized to passive radius.

under passive conditions at the mean ventral aortic pressure, the incremental elastic modulus (E_{inc}) appeared to be higher in the mesenteric artery, suggesting increased wall stiffness.

The DNA content of the uterine artery from fish in early pregnancy (candle stage) was higher than that found in the mesenteric and rectal gland arteries (Table 2). In late pregnancy this difference had disappeared. RNA content Table 2.--DNA and RNA Content of Arterial Segments (ug/mg wet wt)

	DNA ug/mg wet wt	RNA ug/mg wet wt	RNA DNA	Dry wt Wet wt
Early Pregnancy (candle stage)				
mesenteric	2.64 ± 1.41 (2)	$1.32 \pm .26$	$.63 \pm .33$	
uterine	$5.01 \pm .05$ (2)*	$2.16 \pm .85$	$.60 \pm .16$	$.27 \pm .05$ (2)
rectal gland	$2.86 \pm .01$ (2)	$1.93 \pm .07$	$.70 \pm .28$	
Late Pregnancy (fetus present)				
mesenteric	$1.93 \pm .50$ (4)	$1.96 \pm .24$	$1.15 \pm .24$	$.38 \pm .08$ (3)
uterine	$2.76 \pm .45$ (4)	$2.09 \pm .33$	$.84 \pm .14$	$.34 \pm .05$ (4)
rectal gland	$2.97 \pm .19$ (3)	$2.17 \pm .24$	$.75 \pm .12$	

* $p < .01$

of all three arteries from fish in early pregnancy were comparable to those found in fish in later pregnancy. Water content of the uterine artery appeared to decrease in late pregnancy.

Discussion

The mechanics of pregnant dogfish arteries are similar to those measured in mammalian systemic arteries. The ratio of the radius at maximal pressure to the radius at zero pressure (r_{max}/r_o) found in the dogfish, 1.8-2.0 (Table 1) is only slightly higher than the 1.6 found in the canine iliac artery (Cox, RH, Am. J. Physiol. 230:462-470, 1976). However, the maximal circumferential stress is an order of magnitude lower (10^+5 dynes/cm²) than that found in mammals (10^+6 dynes, cm²). This is not unexpected in view of the low arterial pressure found in the ventral and dorsal aortas.

The high DNA content of the uterine artery found in early pregnancy (Table 2) suggests that this artery is undergoing growth. The decrease in DNA content in late pregnancy could be due to a decrease in the number of cells or to a relative increase in the non-nuclear constituents of existing cells. Since a decrease in the number of cells is unlikely, the data indicate that growth has continued into late pregnancy. In the absence of information on the number of cells relative to DNA content, it is not possible to determine whether growth took place by hyperplasia or by hypertrophy. Gestational processes, however, do not appear to affect the other systemic arteries.

The growth indicated by the biochemical measurements is reflected by mechanical measurements. The uterine artery during late pregnancy has a thicker wall (lower r/h value) and is more compliant (higher E_{inc}) than the mesenteric artery. Furthermore, measurements on uterine arteries from non-pregnant dogfish are needed to substantiate these conclusions. The authors acknowledge the assistance of Michael Levy and Francisco Bonilla in obtaining the tissues and Gwen Lech for help with biochemical analyses. This work was supported in part by NIH Grant HD 16899, and by research funds from the Department of Surgery, Mt. Sinai School of Medicine, New York, N.Y., 10029.

THE SIGNIFICANCE OF VASODILATION IN THE SECRETORY RESPONSE OF THE RECTAL GLAND

T.J. Shuttleworth and J.L. Thompson, Department of Biological Sciences, University of Exeter, Exeter, England

Whilst various hemodynamic changes associated with the stimulation of secretion in the rectal gland have been described (Solomon et al., Bull. MDIBL 20:138-141, 1980; Shuttleworth, J. Exp. Biol., 103:193-204, 1983), the physiologically significant parameters have never been specifically defined or their importance in the overall secretory response assessed. The purpose of this study was to investigate the effects of changes in perfusion pressure, perfusion flow and vascular conductance both singularly and "in concert" on secretion rate in isolated perfused glands from *Squalus*.

Isolated glands were perfused with saline containing dibutyryl cAMP (0.05 mmol l^{-1}) and theophylline (0.25 mmol l^{-1}) using a constant pressure regime, as described previously (Shuttleworth, loc. cit.), and gassed with 99% O_2 :1% CO_2 . The rectal gland vein and the secretory duct were cannulated and the cannulae led to drop sensors connected to a 2-channel microprocessor-controlled flowmeter (recording flow in $\mu\text{l min}^{-1}$). This permitted continuous recording of both efferent perfusion flow and secretion flow. The sodium secretion in the secreted fluid was determined from samples collected from the cannula in the secretory duct and from this, and the recorded secretion flow, sodium secretion rate could be calculated.

Glands were initially perfused at the physiological pressure of 20 mm Hg. Under these conditions, efferent perfusion flow was $2802 \pm 109 \mu\text{l g}^{-1} \text{ min}^{-1}$, secretion concentration (Na) $530.6 \pm 2.3 \text{ mmol l}^{-1}$, and the secretion rate $24.6 \pm 0.9 \mu\text{mol g}^{-1} \text{ min}^{-1}$ (mean \pm S.E., $N=19$ in each case). The effect of changing the afferent perfusion pressure (by raising or lowering the perfusion head) is shown in Figure 1. It is clear that, at perfusion pressures below those normally found in vivo, secretion rate is significantly reduced whilst the concentration of the secreted fluid is maintained. Supranormal pressures however produce only a relatively small increase in secretion rate - an effect apparently limited by a concomitant reduction in the concentration of the secreted fluid. As this represents a reduction in the concentration gradient between the secretion and the perfusion fluid and is accompanied by an increase in the volume of fluid secreted, it probably indicates the onset of damage to the integrity of the epithelium induced by pressures in excess of the physiological range.

Despite the clear effect of a reduced perfusion pressure on secretion rate shown in Figure 1, it must be remembered that other hemodynamic parameters are effected by lowering the afferent perfusion pressure head. Most notable among these is the simultaneous reduction in perfusion flow. In order to investigate whether the observed fall in secretion rate was due to changes in perfusion flow rather than a direct effect of perfusion pressure, experiments were carried out where perfusion flow was reduced whilst maintaining a constant perfusion pressure (20 mmHg).